Nuclear Physics A460 (1986) 181–200
North-Holland, Amsterdam

STRONG M2 TRANSITIONS

F. ZIJDERHAND and C. VAN DER LEUN

Fysisch Laboratorium, Rijksuniversiteit Utrecht, P.O. Box 80.000, 3508 TA Utrecht, Netherlands

Received 7 July 1986

Abstract: The recommended upper limit (RUL) for isospin-allowed M2 γ-ray transition strengths is largely determined by the strongest observed M2 transitions. In order to check this M2 RUL the strengths of the five strongest reported primary M2 transitions have been remeasured via (p, γ) reactions. The results are:

^{14}N,	$E_x = 8.91 \rightarrow 0$ MeV:	2.2 ± 0.3 W.u.;
^{16}O,	$E_x = 12.97 \rightarrow 0$ MeV:	1.0 ± 0.3 W.u.;
^{16}O,	$E_x = 12.53 \rightarrow 0$ MeV:	1.12 ± 0.17 W.u.;
^{21}Na,	$E_x = 2.80 \rightarrow 0.33$ MeV:	<0.4 W.u.;
^{32}S,	$E_x = 10.08 \rightarrow 0$ MeV:	0.93 ± 0.13 W.u.

Although all but one of these new M2 strengths are lower than the previously reported values, the M2 RUL of 3 W.u. for nuclei with $A = 6-44$ cannot be reduced due to the strong transition in ^{14}N.

E

NUCLEAR STRUCTURE ^{13}C(p, γ), $E \approx 1460$ keV; ^{15}N(p, γ), $E \approx 430$, 900 keV; ^{20}Ne(p, γ), $E \approx 380$ keV; ^{31}P(p, γ), $E \approx 1250$ keV; measured $\sigma(E, E_\gamma)$. ^{14}N, ^{16}O, ^{21}Na, ^{32}S deduced resonance strengths, γ-ray branching ratios, Γ_γ, Γ_p, Γ_α, Γ, T. Enriched targets, implanted targets.

1. Introduction

Ever since the early days of γ-ray spectroscopy, spins, parities and isospins have been assigned to nuclear levels on the basis of what are considered impossible, unacceptable or improbable γ-ray transition strengths. It was a generally accepted and fruitful tool in nuclear structure studies. A large variety of different limits for acceptability, however, was used in different publications. To remedy this lack of uniformity, Endt and Van der Leun proposed [1]) in 1974 a set of recommended upper limits (RUL's) for the strength of γ-ray transitions in the sd-shell nuclei. The upper limits are defined as the values which are exceeded with a probability of at most 0.1%.

The first set of RUL's has been updated and extended to lighter and heavier nuclei in a series of papers by Endt [2,3]). These RUL's have found broad acceptance; they are e.g. incorporated in the list of strong arguments for spin and parity assignments printed in each issue of the Nuclear Data Sheets.

This paper concentrates on one of the most frequently quoted RUL's: that for isospin-allowed M2 transitions in $A = 6-44$ nuclides. The most recent published value for this isovector M2 RUL is $S_{M2} = 3$ W.u. [ref. [2])]; it is based on the strongest observed M2 transitions. Table 1 lists the transitions with a reported M2 strength $S_{M2} > 1$ W.u. The highest M2 strength listed, for the $7.80 \rightarrow 0$ MeV transition in ^{35}Cl,

has been shown [4]) to be incorrect; it is based on an erroneous spin assignment to the $E_x = 7.80$ MeV level. In line with this finding, it was considered worthwhile to remeasure the strengths of the strongest reported M2 transitions. There are three reasons why such a check is justified.

(i) Relative to the accompanying E1 and M1 transitions, the M2 transitions are in general rather weak. Therefore special attention has to be paid to possible background contributions and instrumental effects. As will be shown in this paper, the effect of the total dead time of the electronics for instance may be of significant importance.

(ii) Several of the strengths listed in table 1 have been deduced only from (e, e') experiments in which the energy resolution was not sufficient to clearly resolve the studied transitions. Furthermore the analysis of these experiments is not fully model-independent.

(iii) Several strengths were found as a byproduct in experiments aiming at other data.

The present experiments focus on the strength of five primary M2 transitions from proton-capture resonance levels; see table 1. The general experimental method is described in sect. 2. Sects. 3 to 7 describe the separate M2 strength measurements and in sect. 8 the results are summarized and discussed. This paper supersedes the preliminary publication of this experiment in ref. [7]).

TABLE 1

Previously observed M2 transitions with $S_{M2} > 1$ W.u.

Nucleus	$E_{xi} \rightarrow E_{xf}$ (MeV)	$J_i^\pi \rightarrow J_f^\pi$	S_{M2} (W.u.) [a])
^{14}N	8.91 → 0	$3^- \rightarrow 1^+$	1.4 ± 0.5
^{16}O	12.53 → 0	$2^- \rightarrow 0^+$	0.7 ± 0.2 [b]) or 3.7 ± 0.5 [c])
^{16}O	12.97 → 0	$2^- \rightarrow 0^+$	2.0 ± 0.1
^{21}Na	2.80 → 0.33	$\frac{1}{2}^- \rightarrow \frac{5}{2}^+$	1.1 ± 0.4
^{22}Ne	7.60 → 0	$2^- \rightarrow 0^+$	1.6 ± 0.4
^{32}S	10.08 → 0	$2^- \rightarrow 0^+$	1.3 ± 0.4
^{34}S	5.68 → 2.13	$2^- \rightarrow 2^+$	1.1 ± 0.4
^{35}Cl	7.80 → 0	$\frac{3}{2}^- \rightarrow \frac{3}{2}^+$	3.1 ± 1.0

[a]) From the review given in ref. [2]), unless indicated otherwise.
[b]) Ref. [6]).
[c]) Ref. [5]).

2. Set-up and method

2.1. EXPERIMENTAL SET-UP

The proton beam used in the present experiments is produced by the Utrecht 3 MV Van de Graaff accelerator [8]). A 90° analysing magnet with stabilising slits

leads to a proton-energy resolution $\Delta E_p \approx 200$ eV at $E_p = 1$ MeV. Beam currents are used ranging from 5 up to 150 μA on target, depending on target stability and/or counting rate requirements. The vacuum in the beam lines and the target chamber is better than 10^{-6} Torr. A liquid-nitrogen cooling trap is positioned in front of the target to reduce the build-up of contaminants on the target.

The targets used are described below per experiment; they had backings of 0.3 mm thick tantalum, unless indicated otherwise. The amount of fluorine and sodium contamination in these backings is reduced by heating them in vacuum to about 1700 K for about 5 min, before depositing the target material.

The size of the beam spot on the target is normally less than 2×2 mm^2. To reduce local heating and thus deterioration, the targets are directly water-cooled and in most cases the proton beam is wobbled up-and-down over a range of 10 mm. Targets are replaced after a reduction of the γ-ray yield of typically 30%.

In the measurements to be discussed below, one hyperpure n-type Ge detector and four Ge(Li) detectors are used, with active volumes of about 100 cm^3 and γ-ray energy resolutions between 1.8 and 2.1 keV at a γ-ray energy of $E_\gamma = 1.33$ MeV. The γ-ray efficiency curves ($E_\gamma = 0.2 - 13$ MeV) of these detectors are measured with the radioactive sources ^{56}Co, ^{110m}Ag, ^{133}Ba, ^{152}Eu and ^{226}Ra [ref. [9])] and the proton-capture resonances at $E_p = 767$ and 1317 keV in ^{27}Al(p, γ)^{28}Si, at $E_p = 1020$, 1317 and 1417 keV in ^{23}Na(p, γ)^{24}Mg and at $E_p = 675$ and 1388 keV in ^{11}B(p, γ)^{12}C [ref. [10])]. Lead absorbers of 5 mm thick have been positioned in front of the detectors to reduce the number of low-energy γ-rays and thus the counting rate. The corresponding corrections are calculated [26]) and applied to the deduced efficiency curves. The detectors used were positioned at a target-to-detector distance of $D = 4$ cm and at $\theta = 55°$ with respect to the proton beam direction to minimize the effect of the angular distributions on the measured γ-ray yields. Spectra of 8192 channels are accumulated in a computer memory via a DMI interface and dumped on tape for off-line analyiss.

2.2. MEASUREMENTS

The intensities of the M2 transitions discussed in this paper are weak compared to those of the competing primaries of lower multipolarity of the (p, γ) resonances studied. Therefore special attention is given to the measurement of γ-ray branching ratios. In contrast to the ^{35}Cl experiments mentioned above, the spins and parities of the states involved in the transitions studied here are well established [11-13]) and will be considered to be correct in this paper.

The general experimental procedure was as follows.

- Determination of the shape of the resonance and its background. A yield curve is measured over the resonance. At each proton energy a spectrum is recorded and analysed off-line for each relevant peak in the spectrum. Possible differences between these yield curves would reveal a multiplet character of the resonance [14]).

- Determination of the branching ratio of the M2 transition. An on-resonance and an off-resonance spectrum are measured with high statistics. In order to determine the resonance decay scheme and thus the branching ratio of the M2 transition studied, the on-resonance γ-ray yield is corrected for the corresponding off-resonance yield.

- Determination of the γ-ray width Γ_γ. The width Γ_γ is deduced from the resonance strength $S = (2J+1)\Gamma_p\Gamma_\gamma/\Gamma$, where J is the resonance spin, Γ_p the proton width and Γ the total width; all widths are given in the center-of-mass system in this paper. This strength is determined by measuring alternately the yield curves of the resonance under investigation and of a calibration resonance. The ratio of the two strengths follows from the ratio of the areas of the resonance peaks in the yield curves, as described in ref. [15]).

2.3. TARGET DETERIORATION, TOTAL DEAD TIME AND SUMMING EFFECTS

As mentioned above, the off-resonance contribution is subtracted from the on-resonance yield. Instrumental effects like target quality, total dead time, and coincident and random summing may, however, be different for the on-resonance and the off-resonance measurements. These differences should be taken into account in the subtraction. The influence of the target deterioration is reduced by alternate on- and off-resonance measurements. Both total dead time and random summing are monitored by recording simultaneously the γ-radiation from the target and the pulses of a pulse generator which was connected to the test-input of the preamplifier.

Experimental conditions like beam current and detector-to-target distance are chosen such that the corrections for total dead time and random summing are limited to at most 10% together and to less than 3% in the $^{13}C(p, \gamma)^{14}N$ measurements, for reasons to be discussed below. The data are corrected for target deterioration, total dead time and random summing, unless indicated otherwise. The effects of coincident summing are sufficiently small. Due to the target-to-detector distances chosen, effects on the M2 strengths are far less than 5%.

3. The $E_x = 8.91 \rightarrow 0$ MeV transition in ^{14}N

The $E_x = 8.91$ MeV state of ^{14}N is the $^{13}C(p, \gamma)^{14}N$ resonance level at $E_p = 1462$ keV with $\Gamma = 16 \pm 2$ keV [ref. [11])]. The measurement of the M2 strength of the $E_x = 8.91 \rightarrow 0$ MeV, $J^\pi = 3^- \rightarrow 1^+$ transition is the subject of this section. In measuring the γ-ray branching ratios of the $E_x = 8.91$ MeV level one has to take into account the yield of the broad $^{13}C(p, \gamma)^{14}N$ resonances at $E_p = 551$ and 1270 keV. The targets used for these experiments are prepared by sputtering 20 to 80 $\mu g/cm^2$, 98.1% enriched ^{13}C onto the backings. At $E_p = 1450$ keV these thicknesses correspond to a proton-energy loss of 4 to 17 keV. The targets withstand beams of 150 μA for more than 20 h with a loss of yield of less than 30%.

3.1. THE $E_p = 1462$ keV RESONANCE

3.1.1. Yield curve. Spectra have been recorded at thirty energies over the $E_p = 1462$ keV resonance in E_p steps of about 4 keV; the collected proton charge amounts to 90 mC per spectrum. In order to check the singlet character of this resonance and to determine the background at $E_p = 1462$ keV, separate yield curves have been deduced from the measured spectra for each relevant γ-line. None of the yield curves shows a significantly different resonance energy or width. The background corrections are less than 10% for all branches except for the ground-state transition. Fig. 1a shows the yield curve of the ground-state transition over the $E_p = 1462$ keV resonance. This figure clearly demonstrates the main problem of the strength measurement: even at the top of the resonance only about 6% of the γ_0 yield is due to the resonance studied (note the suppressed zero), whereas the remainder is primarily due to the broad resonance at $E_p = 1270$ keV.

The data are corrected for total dead time and random summing effects and presented in fig. 1a; the maximum correction amounts to $(3.0 \pm 0.3)\%$ of the total γ_0 yield. At proton energies below and above the resonance these effects are negligible, but on-resonance the decay is strongly dominated by cascade transitions leading to a high counting rate. Consequently a low beam current (25 μA), a large detector-to-target distance ($D = 7$ cm) and a thick lead absorber (25 mm) between

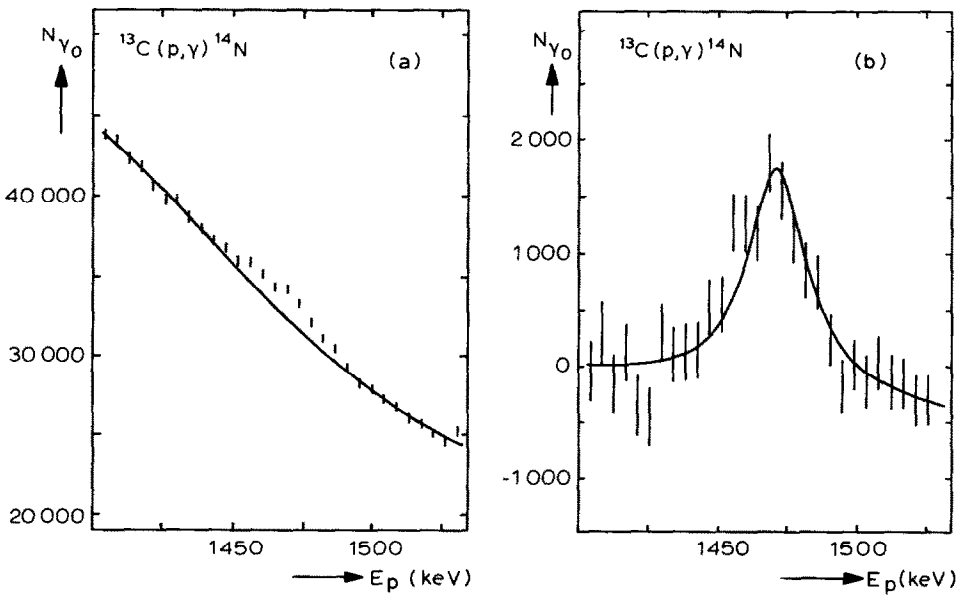

Fig. 1. Yield curves for ground-state γ-rays around the $^{13}C(p, \gamma)^{14}N$ resonance at $E_p = 1462$ keV. The yield is the sum of the contents of the escape and full-energy peaks. (a) The data corrected for total dead time and random summing effects and (b) the data shown in fig. 1a after subtraction of the contribution from the broad resonance at $E_p = 1270$ keV. The drawn lines are explained in the text.

target and detector are used to keep the total dead time and random summing effects below 3%.

The drawn line in fig. 1a is the result of a fit of a Breit-Wigner curve with its top at $E_p = 1270$ keV to the data points below and above the 1462 keV resonance. Subtraction of this background leads to the resonant yield presented in fig. 1b. The drawn line is a least-squares fit of a Breit-Wigner curve plus a linear background. In this fit the position and the width of the Breit-Wigner curve are fixed at the values deduced in a separate fit to the data points of the yield curve of the strong (84%) $r \rightarrow 5.83$ MeV branch of the $E_p = 1462$ keV resonance, which is not observed in the decay of the broad $E_p = 1270$ keV resonance. From the fit shown in fig. 1b one finds that at the maximum of the $E_p = 1462$ keV resonance only $(5.9 \pm 0.5)\%$ of the total observed $r \rightarrow 0$ MeV yield arises from this resonance.

3.1.2. The γ-ray branching ratios. The spectrum measured at the maximum of the yield curve has been used to determine the decay scheme of the $E_p = 1462$ keV resonance. The γ-ray yields are corrected for the background contributions deduced from the yield curves discussed in sect. 3.1.1. This leads to a γ-ray ground-state branch of $(2.9 \pm 0.3)\%$. The branching ratios obtained are given in table 2, together with literature data.

TABLE 2

Parameters of the $^{13}C(p, \gamma)^{14}N$ resonance at $E_p = 1462$ keV

	Present experiment	Literature [a])
$r \rightarrow 0$ MeV branching (%)	2.9 ± 0.3	1.6 ± 0.5 [b])
$\rightarrow 5.11$	4.2 ± 0.5	5 ± 3
$\rightarrow 5.83$	84.3 ± 0.9	89 ± 3
$\rightarrow 6.44$	5.3 ± 0.6	3 ± 1
$\rightarrow 7.03$	3.3 ± 0.5	1.4 ± 0.8
E_p (keV)		1462 ± 3
E_x (keV)		8909.1 ± 1.6
$J^\pi; T$		$3^-; 1$
$S(p, \gamma)$ (eV)	2.7 ± 0.3	2.9
Γ (keV)		16 ± 2
Γ_γ (eV)	0.38 ± 0.04	0.41
Γ_{γ_0} (meV)	11.0 ± 1.7	6.6 ± 2.2
$S_{M2}(r \rightarrow 0)$ (W.u.)	2.2 ± 0.3	1.4 ± 0.5

[a]) Ref. [11]).
[b]) See text.

3.1.3. The resonance strength. The strength of the $E_p = 1462$ keV resonance has been measured relative to the strength of the $^{13}C(p, \gamma)^{14}N$ resonance at $E_p =$ 1748 keV. The latter has been determined recently by Biesiot *et al.* [16]) as $S(1748) =$

43 ± 3 eV. The ratio $S(1462)/S(1748) = 0.062 \pm 0.005$, deduced from the present experiment, then yields $S(1462) = 2.7 \pm 0.3$ eV. With $J = 3$ and $\Gamma \approx \Gamma_p \gg \Gamma_\gamma$ this implies $\Gamma_\gamma = 0.38 \pm 0.04$ eV and thus $\Gamma_{\gamma_0} = 11.0 \pm 1.7$ meV, since we have $\Gamma_{\gamma_0}/\Gamma_\gamma = (2.9 \pm 0.3)\%$.

3.2. THE $E_p = 1270$ keV RESONANCE

In order to determine the nature of the strong background in the $r \to 0$ MeV yield curve around the $E_p = 1462$ keV resonance discussed above, the ground-state transition yield curve has been measured over the range $E_p = 500$ to 2000 keV in steps of 50 keV (see fig. 2a). This shows that the ground-state transition at $E_p = 1462$ keV is mainly due to the $E_p = 1270$ keV resonance.

The observed position and width of the resonance are deduced from fig. 2a as $E_p = 1290 \pm 20$ keV and $\Gamma_{lab} = 430 \pm 20$ keV, respectively. To deduce these values, the data of the yield curve are corrected for the $E_p = 551$ keV contribution and for the variation in the detector efficiency since E_γ depends on E_p. The shape of the resulting yield curve is, however, not exactly a Breit-Wigner form, since the following factors in the cross section vary over the large E_p-range.

(i) The penetrability $P_l(l = 0)$, which is calculated according to ref. [15]), but with a nuclear radius parameter of 1.2 fm.

(ii) The $1/E_p$ factor arising from the λ^2 term in the Breit-Wigner function for the cross section (λ denotes the De Broglie wavelength of the proton).

(iii) The E_γ^3 factor in the dipole γ-ray transition probability.

These corrections are applied before the data are fitted to a Breit-Wigner function plus a linear background. The result of the fit is presented by the drawn line in fig. 2b; the position and width are $E_p = 1273 \pm 10$ keV and $\Gamma_{lab} = 450 \pm 10$ keV, respectively. They do not deviate very much from the results of the raw data. The resulting resonance energy and width, both corrected for the target thickness of 6 keV, are given in table 3.

The strength of the $E_p = 1270$ keV resonance is determined from these data as a byproduct. It results from the ratio of the yield $y(1270)$ at the maximum of the $E_p = 1270$ keV resonance and the area $Y(1462)$ of the yield curve of the $E_p = 1462$ keV resonance, according [15]) to

$$\frac{S(1270)}{S(1462)} = \frac{\pi\, y(1270)\, 1270}{2\, Y(1462)\, 1462}\Gamma(1270).$$

Formally this is restricted to narrow resonances, but the small deviations of position and width between the raw data and the corrected data show that this formula can be applied here. With $J = 0$, $\Gamma \approx \Gamma_p \gg \Gamma_\gamma$ and $\Gamma_{\gamma_0}/\Gamma_\gamma = (90 \pm 10)\%$, this leads to $S(1270) = 32 \pm 7$ eV and to $\Gamma_\gamma = 32 \pm 7$ eV.

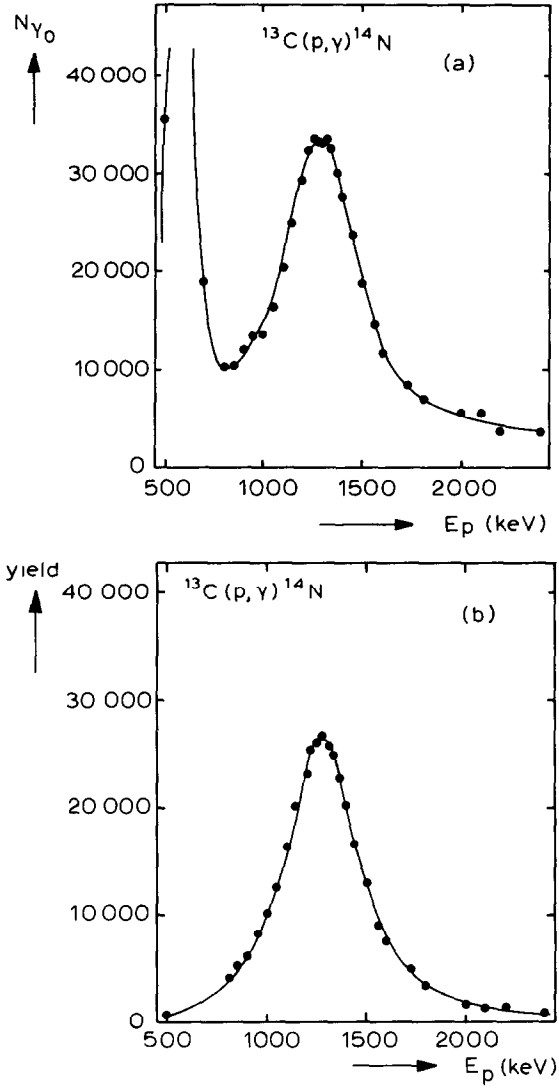

Fig. 2. Yield curves of $^{13}C(p, \gamma)^{14}N$ ground-state γ-rays in the $E_p = 500$–2500 keV region. The γ-ray yields are deduced from the full-energy peaks. (a) The raw data and (b) the data after correction for the contribution of the $E_p = 551$ keV resonance and for several E_p dependent factors (see text).

3.3. DISCUSSION

The main goal of the measurements described in this section is the M2 strength of the ground-state transition of the $E_x = 8.91$ MeV level of ^{14}N. The result of this experiment is $S_{M2}(r \to 0) = 2.2 \pm 0.3$ W.u., somewhat higher than the value $S_{M2} = 1.4 \pm 0.5$ W.u. which results from $\Gamma_{\gamma_0} = 6.6 \pm 2.2$ meV measured by Clerc *et al.* [17]) in an (e, e') experiment. The $r \to 0$ MeV branching ratio of $(1.6 \pm 0.5)\%$ listed by

TABLE 3

Parameters of the $^{13}C(p, \gamma)^{14}N$ resonance at $E_p = 1270$ keV

	Present experiment	Literature [a])
E_p (keV)	1270 ± 10	1340 ± 50
E_x (keV)	8730 ± 10	8790 ± 50
J^π; T		0^-; 1
$S(p, \gamma)$ (eV)	32 ± 7	51 ± 13
Γ (keV)	418 ± 10	≈ 460
Γ_{γ_0} (eV)	29 ± 6	46 ± 12
$r \rightarrow 0$ MeV branching (%)		90 ± 10

[a]) Ref. [11]).

Ajzenberg-Selove [11]) is based on this (e, e') result and thus is not directly comparable with the ratio of (2.9 ± 0.3)% from the present experiment.

Tables 2 and 3 summarise the results of the measurements at the $^{13}C(p, \gamma)^{14}N$ resonances at $E_p = 1462$ and 1270 keV, respectively. Apart from the discrepancy mentioned above, the overall agreement with previous data is good.

4. The $E_x = 12.97 \rightarrow 0$ MeV transition in ^{16}O

The M2 strength of the $E_x = 12.97 \rightarrow 0$ MeV, $J^\pi = 2^- \rightarrow 0^+$ transition in ^{16}O is discussed in this section. The $E_x = 12.97$ MeV level is populated in the $^{15}N(p, \gamma)^{16}O$ resonance at $E_p = 897$ keV [ref. [12])]. The decay of this level is heavily dominated by α-decay to the first excited state of ^{12}C at $E_x = 4.44$ MeV, which in turn decays to the ^{12}C ground-state by γ-ray emission. Because of the high intensity of these 4.44 MeV γ-rays, extra care has to be paid to total dead-time and random-summing effects.

4.1. MEASUREMENTS AND RESULTS

4.1.1. Yield curve and decay scheme. The target used is made by implantation in tantalum of N^+ ions, 11.7% enriched in ^{15}N, at $E(N^+) = 3$ keV. A yield curve is measured repeatedly over the range $E_p = 888$–910 keV in steps of ≈1 keV. Two Ge(Li) detectors are used and a proton charge of 860 mC is collected per measuring point. Yield curves for each capture γ-ray transition and for the $E_\gamma = 4.44$ MeV, $(p, \alpha_1\gamma)$ transition, are deduced from these data. Only the $E_x = 6.13 \rightarrow 0$ and the $r \rightarrow 0$ MeV transitions show a significant off-resonance yield, with off-resonance to on-resonance yield ratios of 0.11 ± 0.03 and 0.34 ± 0.06, respectively. The off-resonance yield of the 6.13 MeV γ-ray is due to the well known $^{19}F(p, \alpha_2\gamma)^{16}O$ background reaction. The off-resonance yield of the $E_\gamma = 12.97$ MeV ground-state transition arises from the broad ($\Gamma = 140$ keV) $^{15}N(p, \gamma)^{16}O$ resonance at $E_p = 1028$ keV

[ref. [12])]. One finds that only $(66 \pm 6)\%$ of the $E_\gamma = 12.97$ MeV on-resonance yield is due to the $E_p = 897$ keV resonance.

The decay scheme of the $E_p = 897$ keV resonance is determined from the on-resonance data, taking into account the background contributions mentioned above. Table 4 lists the deduced branching ratios and compares them to literature data. The yield of the 4.44 MeV γ-ray is equivalent to the α_1 decay yield. Comparison of this yield with the γ-decay yield of the $E_x = 12.97$ MeV level implies a ratio $\Gamma_\gamma/\Gamma_{\alpha_1} = (5.48 \pm 0.16) \times 10^{-3}$.

TABLE 4

Parameters of the $^{15}N(p, \gamma)^{16}O$ resonance at $E_p = 897$ keV

	Present experiment	Literature [a])
$r \rightarrow 0$ MeV branching (%)	2.1 ± 0.4	1.9 ± 0.1 [b])
$\rightarrow 6.13$	50 ± 2	63 ± 6
$\rightarrow 7.12$	6 ± 1	12 ± 3
$\rightarrow 8.87$	42 ± 2	25 ± 3
E_p (keV)		897.4 ± 0.3
E_x (keV)		12968.5 ± 0.4
$J^\pi; T$	$; 1+0$	$2^-; 1$
$S(p, \alpha_1)$ (keV)	1.17 ± 0.15	2.2 [b])
$S(p, \gamma)$ (eV)	6.4 ± 0.8	12 [b])
Γ (keV)	1.34 ± 0.04	1.59 ± 0.12 [c])
Γ_{α_1} (keV)	0.30 ± 0.06	0.60 ± 0.07 [c])
Γ_p (keV)	1.04 ± 0.07	0.99 ± 0.12 [c])
Γ_γ (eV)	1.6 ± 0.3	3.8 ± 0.2
Γ_{γ_0} (meV)	34 ± 9	71 ± 2
$S_{M2}(r \rightarrow 0)$ (W.u.)	1.0 ± 0.3	2.0 ± 0.1 [b])

a) Ref. [12]), unless indicated otherwise.
b) Calculated from the values listed in the last column.
c) Ref. [21]).

4.1.2. The resonance strength. The (p, γ) resonance strength S equals $S_{\alpha_1}\Gamma_\gamma/\Gamma_{\alpha_1}$ where $S_{\alpha_1} = (2J+1)\Gamma_p\Gamma_{\alpha_1}/\Gamma$ is the (p, α_1) strength. The strong $\alpha_1\gamma$ decay was used to measure S_{α_1}, from which S can be deduced with the measured $\Gamma_\gamma/\Gamma_{\alpha_1}$ ratio. The measurement of S_{α_1} is performed with a 15 μg/cm^2 and an 18 μg/cm^2 Al-N target, both on a 40 μg/cm^2 carbon foil. The low-A backing is chosen because it allows Rutherford back-scattering (RBS) analysis of the targets. These targets are prepared by sputtering aluminium onto the C-foils with beams of N^+ ions from natural nitrogen gas (the ^{15}N abundance is only 0.37%). Since the C-backing could not be water-cooled, the proton-beam currents had to be limited to 5 μA. Yield curves of the $^{15}N(p, \alpha_1\gamma)^{12}C$ resonance at $E_p = 897$ keV and the $^{27}Al(p, \gamma)^{28}Si$ resonance at $E_p = 992$ keV have been measured alternately.

The Al-to-N ratios of the two targets have been determined with RBS with an accuracy of about 5%, both before and after the yield-curve measurements. The

RBS spectra indicate that these Al-N targets also contain 0-atoms. Fresh targets have Al:N:0 atom ratios of about 7:1:3. In the second RBS measurement the targets are scanned over the beam spot of the yield-curve measurement. The results show that during the yield curve experiment, the number of Al and N nuclei in the target-spot area decreased by 5 and 22%, respectively.

The average of the strength ratios measured with the two targets amounts to $S_{\alpha_1}(897)/S(992) = 51 \pm 6$ and implies $S_{\alpha_1} = 1.17 \pm 0.15$ keV, since $S(992) = 22.9 \pm 1.3$ eV [ref. [19])]. Combination with $\Gamma_\gamma/\Gamma_{\alpha_1} = (5.48 \pm 0.16) \times 10^{-3}$ then leads to $S = 6.4 \pm 0.8$ eV.

4.1.3. The total width. Determination of Γ_γ from the resonance strength is not directly possible, since in this case $\Gamma = \Gamma_p + \Gamma_\alpha$ (Γ_γ may be neglected and $\Gamma_\alpha = \Gamma_{\alpha_1}$ [ref. [12])]). Therefore Γ is determined in a separate experiment by measuring the shape of the front edge of a thick-target yield curve. Yield curves of the $^{15}N(p, \alpha_1\gamma)^{12}C$ resonance at $E_p = 897$ keV and the $^{27}Al(p, \gamma)^{28}Si$ resonance at $E_p = 992$ keV are measured with a 15 $\mu g/cm^2$ thick Al-N target on a 0.3 mm thick tantalum backing. The Al resonance serves to measure the instrumental resolution, which is essentially determined by the proton-energy resolution and the target surface inhomogeneities. This instrumental resolution is deduced in the following way. The observed interquartile range of the $E_p = 992$ keV yield curve is 290 ± 30 eV. Correction for the finite width of the resonance, $\Gamma = 100 \pm 15$ eV [ref. [13])], leads to an instrumental width of 230 ± 30 eV. The shape of the instrumental function is assumed to be gaussian, whereas the resonance cross section has a Breit-Wigner shape. The corrections are calculated with the relation [20]) $\Gamma_{BW} = \Gamma_V - \Gamma_G^2/\Gamma_V$ with Γ_{BW}, Γ_V and Γ_G the widths of the Breit-Wigner, the Voigt and the Gauss curves.

An integrated Breit-Wigner shape has been fitted to the data points of the $E_p = 897$ keV resonance, resulting in $\Gamma_{lab} = 1.47 \pm 0.04$ keV (see fig. 3). Corrected for the instrumental width and transformed to the center-of-mass system this leads to $\Gamma = 1.34 \pm 0.04$ keV.

4.1.4. The partial widths. Since $\Gamma = \Gamma_p + \Gamma_{\alpha_1}$, the strength S_{α_1} may be expressed as $(2J+1)(\Gamma - \Gamma_x)\Gamma_x/\Gamma$, where Γ_x equals either Γ_p or Γ_{α_1}. This leads to $\Gamma_x = 0.30 \pm 0.06$ or 1.04 ± 0.07 keV. No *a priori* choice for Γ_p and Γ_{α_1} can be made, but since Γ_p is known [12]) to be larger than Γ_{α_1}, we conclude that our data imply $\Gamma_{\alpha_1} = 0.30 \pm 0.06$ keV and $\Gamma_p = 1.04 \pm 0.07$ keV.

The ratio $\Gamma_\gamma/\Gamma_{\alpha_1} = (5.48 \pm 0.16) \times 10^{-3}$ then leads to $\Gamma_\gamma = 1.6 \pm 0.3$ eV. Combined with the present ground-state branching ratio of $(2.1 \pm 0.4)\%$ this leads to $\Gamma_{\gamma_0} = 34 \pm 9$ meV and thus to $S_{M2}(r \to 0\ \text{MeV}) = 1.0 \pm 0.3$ W.u. for this pure M2 transition.

4.2. DISCUSSION

The present value $S_{M2}(r \to 0\ \text{MeV}) = 1.0 \pm 0.3$ W.u. deviates significantly from the values $S_{M2} = 2.0 \pm 0.1$ W.u. and 2.2 ± 0.5 W.u. deduced from (e, e') experiments reported by Kim *et al.* [5]) and Stroezel *et al.* [6]), respectively. Both experiments, however,

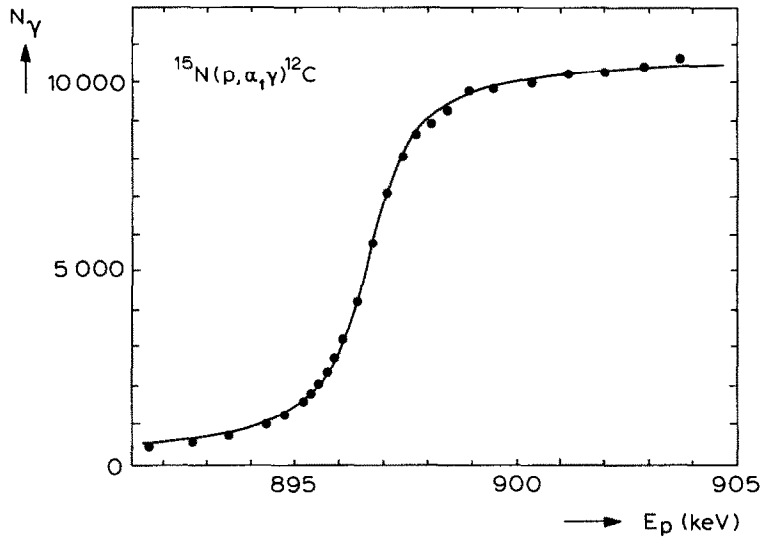

Fig. 3. Thick-target yield curve of the $^{15}N(p, \alpha_1)^{12}C$ resonance at $E_p = 897$ keV for $E_\gamma = 3.0$-4.5 MeV. The drawn line is an integrated Breit-Wigner shape fitted to the data.

do not clearly resolve the peaks corresponding to the $E_x = 12.97$, 13.1 and 13.25 MeV levels. Very recently Leavitt *et al.* [21]) have deduced the values $\Gamma_{\alpha_1} = 0.60 \pm 0.09$ keV and $\Gamma_p = 0.99 \pm 0.12$ keV from $^{15}N(p, \alpha)^{12}C$ and $^{15}N(p, p)^{15}N$ experiments, respectively. The latter value agrees well with our value $\Gamma_p = 1.04 \pm 0.07$ keV. For Γ_{α_1}, however, the two values deviate by a factor of two. This discrepancy is most probably due to the fact that Leavitt *et al.* had to subtract from the (p, α_1) peak a strong background of ^{12}C-recoils from the $^{15}N(p, \alpha_0)^{12}C$ reaction.

5. The $E_x = 12.53 \rightarrow 0$ MeV transition in ^{16}O

The measurement of the M2 strength of the $E_x = 12.53 \rightarrow 0$ MeV, $J^\pi = 2^- \rightarrow 0^+$ transition in ^{16}O is similar to that of the M2 strength described in sect. 4. The $E_x = 12.53$ MeV level is excited by the $^{15}N(p, \gamma)^{16}O$ resonance at $E_p = 429$ keV [ref. [12])]. The decay of this resonance is also strongly dominated by α-decay to the first excited state of ^{12}C at $E_x = 4.44$ MeV.

5.1. MEASUREMENTS AND RESULTS

5.1.1. Yield curve and decay scheme. The yield is measured around $E_p = 429$ keV in E_p steps of about 0.4 keV with an implanted ^{15}N target (see sect. 4). The yield curves for the relevant γ-rays peaks show no doublet character and no significant background contribution. The γ-ray branching ratios and the ratio $\Gamma_\gamma/\Gamma_{\alpha_1} = (6.0 \pm 0.3) \times 10^{-3}$ thus follow directly from the on-resonance data. The deduced values are listed in table 5.

5.1.2. Resonance strength. The resonance strength S_{α_1} is measured relative to the $^{15}N(p, \alpha_1)^{12}C$ resonance at $E_p = 897$ keV with $S_{\alpha_1}(897\text{ keV}) = 1.17 \pm 0.15$ keV (see sect. 4). The measured ratio $S_{\alpha_1}(429)/S_{\alpha_1}(897) = 0.058 \pm 0.002$ implies $S_{\alpha_1}(429) = 68 \pm 9$ eV. Combined with the measured ratio $\Gamma_\gamma/\Gamma_{\alpha_1} = (6.0 \pm 0.3) \times 10^{-3}$, this gives a strength $S = 0.41 \pm 0.05$ eV for the $^{15}N(p, \gamma)^{16}O$ resonance at $E_p = 429$ keV.

5.1.3. Partial widths. In order to deduce Γ_{α_1} from the measured resonance strength S_{α_1} one has to know the total width Γ. A width of $\Gamma_{lab} = 900$ eV is given in the review of Ajzenberg-Selove [12]). In the present experiment, however, thick-target yield curves have been measured for several Al-N targets (see sect. 4.1.3) leading to values for Γ which range from 220 ± 30 to 350 ± 30 eV. These values demonstrate that the resonance width is significantly smaller than the value quoted in ref. [12]), and their spread indicates that it is not feasible to measure the width in this way, probably due to inhomogeneities of the target surfaces.

In the course of the present experiment several papers have been published dealing with $\Gamma(E_x = 12.53\text{ MeV})$. Maurel and Amsel [22]) conlcude to $\Gamma = 120 \pm 30$ eV from the shape of a thick-target ($Nb^{15}N$) yield curve in a $^{15}N(p, \alpha_1)^{12}C$ experiment; Damjantschitsch *et al.* [23]) deduce $\Gamma = 123 \pm 12$ eV from the inverse reaction $^1H(^{15}N, \alpha)^{12}C$ and Leavitt *et al.* [21]) deduce $\Gamma = 97 \pm 10$ eV from the values $\Gamma_p = 25 \pm 3$ eV and $\Gamma_{\alpha_1} = 72 \pm 10$ eV measured in $^{15}N(p, p)^{15}N$ and $^{15}N(p, \alpha)^{12}C$ experiments, respectively. In the present calculation the mean value $\Gamma = 108 \pm 10$ eV will be used.

TABLE 5

Parameters of the $^{15}N(p, \gamma)^{16}O$ resonance at $E_p = 429$ keV

	Present experiment	Literature [a])
$r \to 0$ MeV branching (%)	6.0 ± 0.6	
$\to 6.13$	49 ± 2	60 ± 6
$\to 6.92$	<1	<10
$\to 7.12$	12.0 ± 0.7	15 ± 3
$\to 8.87$	33 ± 2	25 ± 3
E_p (keV)		429 ± 1
E_x (keV)		12530 ± 1
J^π; T	; 1 + 0	2^-; 0
$S(p, \alpha_1)$ (eV)	68 ± 9	83 ± 17 [d])
$S(p, \gamma)$ (eV)	0.41 ± 0.05	0.42 ± 0.07
Γ (eV)		108 ± 10 [b])
Γ_p (eV)	16 ± 3	25 ± 3 [c])
Γ_{α_1} (eV)	92 ± 10	72 ± 10 [c])
Γ_γ (eV)	0.55 ± 0.06	0.36 ± 0.03
Γ_{γ_0} (meV)	33 ± 5	21 ± 6 or 108 ± 15
$S_{M2}(r \to 0)$ (W.u.)	1.12 ± 0.17	0.7 ± 0.2 or 3.7 ± 0.5

[a]) Ref. [11]), unless indicated otherwise.
[b]) See text.
[c]) Ref. [21]).
[d]) Calculated from the values listed in the last column.

Combination of this value with the resonance strength $S_{\alpha_1} = (2J+1)(\Gamma - \Gamma_x)\Gamma_x/\Gamma = 68 \pm 9$ eV results in $\Gamma_x = 16 \pm 3$ or 92 ± 10 eV. Comparison with the literature data then leads to the choice $\Gamma_p = 16 \pm 3$ eV and $\Gamma_{\alpha_1} = 92 \pm 10$ eV. The α_1 width agrees with the value reported by Leavitt *et al.*, whereas the proton width is somewhat lower.

The ratio $\Gamma_\gamma/\Gamma_{\alpha_1}$ combined with our value $\Gamma_{\alpha_1} = 92 \pm 10$ eV results in $\Gamma_\gamma = 0.55 \pm 0.06$ eV. The present ground-state branching ratio then implies $\Gamma_{\gamma_0} = 33 \pm 5$ meV and thus $S_{M2}(r \to 0 \text{ MeV}) = 1.12 \pm 0.17$ W.u.

5.2. DISCUSSION

The present experiment yields $S_{M2}(12.53 \to 0) = 1.12 \pm 0.17$ W.u. This value is in agreement with only one of the values $S_{M2} = 0.7 \pm 0.2$ and 3.7 ± 0.5 eV published by Stroezel [6]) and Kim *et al.* [5]), respectively. In the analysis the literature value $\Gamma(12.53 \text{ MeV}) = 108 \pm 10$ eV has been used; it is the weighted mean from three reported [21-23]) values for Γ measured with quite different techniques. The resulting proton and α-particle widths agree reasonably well with the values reported by Leavitt *et al.* [21]).

Isospins $T = 0$ and $T = 1$ have been assigned [12]) to the $J^\pi = 2^-$, $E_x = 12.53$ and 12.97 MeV levels of ^{16}O, respectively. In a self-conjugated nucleus like ^{16}O a J^π; $T = 2^-$; $0 \to 0^+$; 0 transition is, however, strongly retarded. Since the ground-state transitions from the $E_x = 12.53$ and 12.97 MeV levels are of considerable strengths, the two levels are most probably strongly mixed $T = 0 + 1$ states.

The sum of the presently measured M2 strengths of the two ^{16}O levels agrees with the calculations by Van Hees [18]), who obtained a total strength of 5 W.u. for the two levels while the total experimental strength is 2.1 ± 0.3 W.u.

6. The $E_x = 2.80 \to 0.33$ MeV transition in ^{21}Na

The ^{20}Ne(p, γ)^{21}Na, $E_p = 384$ keV resonance corresponds to the $E_x = 2.80$ MeV, $J^\pi = \frac{1}{2}^-$ state of ^{21}Na. This section describes a measurement of the strength of the $r \to 0.33$ MeV, $J^\pi = \frac{1}{2}^- \to \frac{5}{2}^+$ transition.

The ^{20}Ne targets are prepared by implanting natural neon (^{20}Ne abundance 90.5%) in tantalum backings at $E(Ne^+) = 10$ keV. They withstand molecular H_2^+ beams of about 50 μA for more than 20 h.

6.1. MEASUREMENTS AND RESULTS

The yield at this resonance, with $S(384) = 0.22 \pm 0.04$ meV [ref. [13])], is extremely low. In order to reduce the background from contaminant reactions (mainly on carbon), the target holder, cooling trap and parts of the beam line have been cleaned

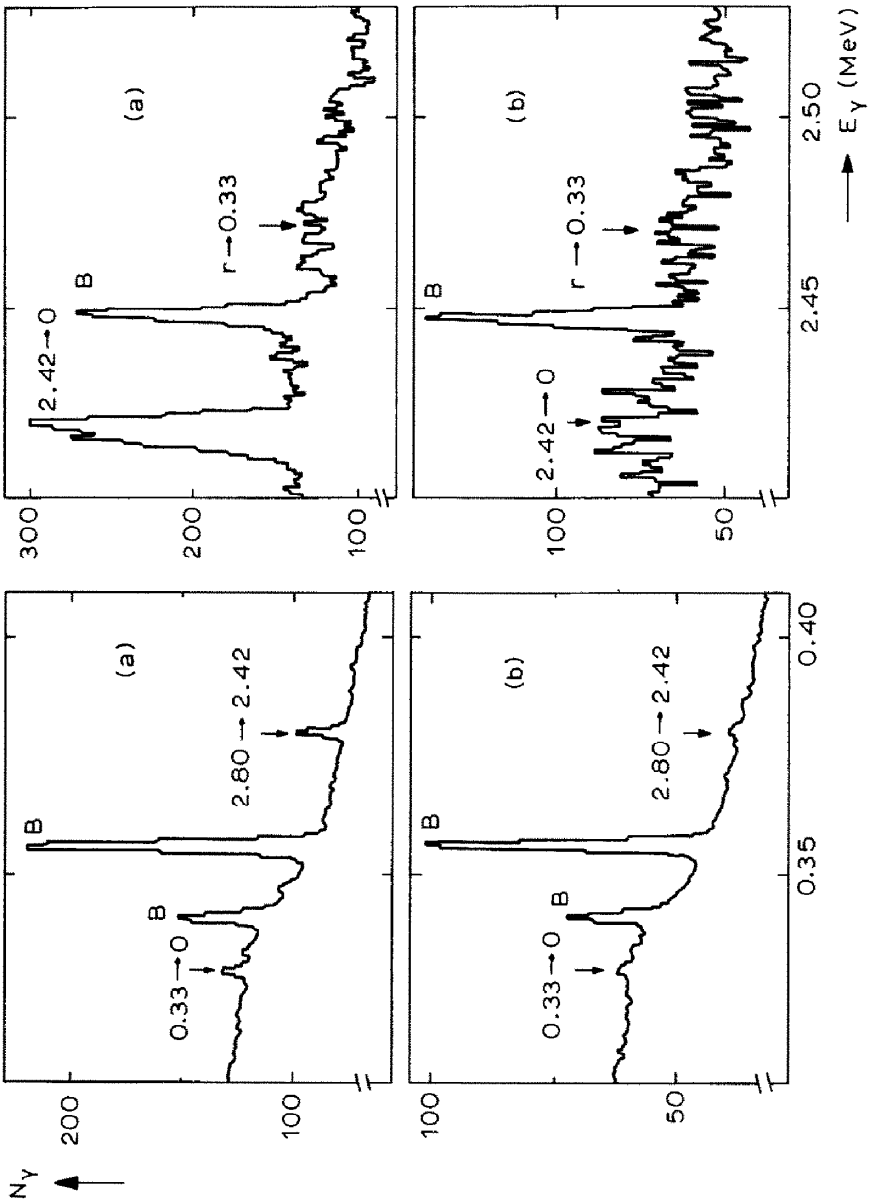

Fig. 4. Relevant parts of the γ-ray spectra measured at the $E_p = 384$ keV, $^{20}Ne(p, \gamma)^{21}Na$ resonance. (a) The sum of the on-resonance spectra (the total collected proton charge is 8.6 C) and (b) the summed off-resonance data (5.0 C). Transition energies are indicated in MeV. Background peaks are indicated by B.

and baked out for several hours at a temperature of about 400 K. In this way the background could be reduced by approximately a factor of ten.

The ^{20}Ne(p, γ)^{21}Na yield curve is deduced from spectra measured at seven proton energies around $E_p = 384$ keV in E_p steps of about 1 keV, with three Ge(Li) detectors placed as close to the target as possible, at $D = 2.5$ cm. The angles at which the detectors are positioned are not relevant here; the γ-ray emission is isotropic since $J = \frac{1}{2}$. Four targets have been used in a total measuring time of about 120 h. Spectra recorded during different runs, on different targets and with different detectors, but at the same proton energy, are summed after matching of zero point and gain of the γ-ray spectra. Although the statistics of these summed spectra are still rather poor, the on- and off-resonance spectra are clearly different. Sum spectra are made of four on-resonance and of three off-resonance spectra; fig. 4 shows the significant parts of these two sum spectra.

The branching ratios deduced from the sum spectra are given in table 6. The yield of the $r \rightarrow 0.33$ MeV (the M2 transition under investigation) and $0.33 \rightarrow 0$ MeV transitions do not differ significantly from zero after subtraction of the off-resonance yield.

The ensuing upper limit for the $r \rightarrow 0.33$ MeV branching is 4%. The clear $E_\gamma = 0.33$ MeV peak in the off-resonance spectrum (see fig. 4b) is most probably due to direct capture [24]). The peak of the DC $\rightarrow 0.33$ MeV, $E_\gamma = 2.47$ MeV transition is broadened in the off-resonance spectrum, since this spectrum is the sum of three spectra taken at different proton energies below and above the resonance energy.

The resonance strength $S = 0.22 \pm 0.04$ meV with $\Gamma > 4.4$ meV [ref. [13])] implies $\Gamma_p \gg \Gamma_\gamma$. Consequently, a γ-ray width $\Gamma_\gamma = 0.11 \pm 0.02$ meV may be deduced from the resonance strength. Combination with the mentioned branching ratio for the $r \rightarrow 0.33$ MeV transition results in $\Gamma_{\gamma_1} < 4$ μeV.

TABLE 6

Parameters of the ^{20}Ne(p, γ)^{21}Na resonance at $E_p = 384$ keV

	Present experiment	Literature [a])
$r \rightarrow 0$ MeV branching (%)	56 ± 5	33 ± 4
$\rightarrow 0.33$	<4	11 ± 4
$\rightarrow 1.72$	<8	<5
$\rightarrow 2.42$	44 ± 5	56 ± 4
E_p (keV)		384 ± 5
E_x (keV)		2798.2 ± 0.8
J^π		$\frac{1}{2}^-$
S(p, γ) (meV)		0.22 ± 0.04
Γ (meV)		>4.4
Γ_γ (meV)		0.11 ± 0.02 [b])
Γ_{γ_1} (μeV)	<4	12 ± 4 [b])
$S_{M2}(r \rightarrow 0.33)$ (W.u.)	<0.4	1.1 ± 0.4 [b])

[a]) Ref. [13]).

[b]) Calculated from the values listed in the last column.

6.2. DISCUSSION

The upper limit $\Gamma_{\gamma_1} < 4$ μeV implies $S_{M2} < 0.4$ W.u., to be compared with $S_{M2} = 1.1 \pm 0.4$ W.u. reported by Rolfs *et al.* [24]). The latter value for the M2 strength is most probably due to an inadequate correction for the significant non-resonant yield from direct capture.

Except for the $r \rightarrow 0.33$ MeV transition mentioned above, the branching ratios listed in table 6 do not deviate strongly from the literature values, except that the present branching ratio of the ground-state transition is somewhat larger than reported previously.

7. The $E_x = 10.08 \rightarrow 0$ MeV transition in ^{32}S

This section describes a measurement of the strength of the $E_x = 10.08 \rightarrow 0$ MeV, $J^\pi = 2^- \rightarrow 0^+$ transition in ^{32}S, which corresponds to the ground-state transition of the ^{31}P(p, γ)^{32}S resonance at $E_p = 1251$ keV.

Targets are prepared by sputtering 10 to 20 μg/cm^2 99.99% pure ^{31}P onto 0.5 mm thick copper backings. These backings have a better heat conductivity than the generally used tantalum backings. This is advantageous since phosphorus targets deteriorate rapidly under bombardment with high proton beam currents; the larger γ-ray background had to be accepted.

7.1. MEASUREMENTS AND RESULTS

Spectra have been measured in small energy steps of about 0.5 keV around $E_p = 1251$ keV. For all relevant peaks a yield curve is determined from these spectra. These curves give no indication of doublet character of the $E_p = 1251$ keV resonance.

The branching ratios have been determined from an on-resonance spectrum measured at $E_p = 1251$ keV and an off-resonance spectrum measured at $E_p = 1234$ keV. For all ^{31}P(p, γ)^{32}S transitions the off-resonance yield is less than 1% of the on-resonance yield. The analysis thus was straightforward. The deduced branching ratios of the $E_x = 10.08$ MeV level are given in table 7.

The strength of the $E_p = 1251$ keV resonance is determined relative to that of the ^{31}P(p, γ)^{32}S resonance at $E_p = 811$ keV, with $S(811) = 1.00 \pm 0.08$ eV [ref. [19])]. The measured ratio $S(1251)/S(811) = 4.3 \pm 0.4$ then leads to $S(1251) = 4.3 \pm 0.5$ eV. The total width $\Gamma = 1.6 \pm 0.2$ keV [ref. [13])] implies $\Gamma_p \gg \Gamma_\gamma$; the measured strength then leads to $\Gamma_\gamma = 0.86 \pm 0.11$ eV and thus to $\Gamma_{\gamma_0} = 1.5 \pm 0.2$ meV, since we have $\Gamma_{\gamma_0}/\Gamma_\gamma = (1.7 \pm 0.1)\%$ from the present experiment.

7.2. DISCUSSION

The value $\Gamma_{\gamma_0} = 1.5 \pm 0.2$ eV results in an M2 strength of $S_{M2}(10.08 \rightarrow 0) = 0.93 \pm 0.13$ W.u., which can be compared to $S_{M2} = 1.3 \pm 0.4$ W.u. from ref. [2]). Table

TABLE 7

Parameters of the $^{31}P(p, \gamma)^{32}S$ resonance at $E_p = 1251$ keV

	Present experiment	Literature
$r \rightarrow 0$ MeV branching (%)	1.7 ± 0.1	2 [a])
$\rightarrow 2.23$	29.6 ± 1.5	34 [a])
$\rightarrow 4.28$	1.5 ± 0.1	2 [a])
$\rightarrow 4.70$	0.7 ± 0.1	(1) [a])
$\rightarrow 5.01$	13.8 ± 0.7	12 [a])
$\rightarrow 5.41$	4.3 ± 0.3	4 [a])
$\rightarrow 6.22$	49 ± 2	45 [a])
E_p (keV)		1251.4 ± 0.6 [b])
E_x (keV)		10076.7 ± 0.8 [b])
$J^\pi; T$		$2^-; 1$ [b])
$S(p, \gamma)$ (eV)	4.3 ± 0.5	5.0 ± 0.4 [c])
Γ (keV)		1.60 ± 0.24 [b])
Γ_γ (eV)	0.86 ± 0.11	0.92 ± 0.12 [d])
Γ_{γ_0} (meV)	1.5 ± 0.2	1.8 ± 0.2 [d])
$S_{M2}(r \rightarrow 0)$ (W.u.)	0.93 ± 0.13	1.3 ± 0.4 [d])

[a]) Ref. [25]).
[b]) Ref. [13]).
[c]) From $S(811) = 1.00 \pm 0.08$ eV [ref. [19])] and $S(1251)/S(811) = 5.0$ [ref. [25])].
[d]) Calculated from the values listed in the last column.

7 summarises the results of the present experiment and compares them with the literature data; the overall agreement is good. The M2 strength is slightly lower than the previous value, but the two values agree within the combined experimental errors.

8. Summary and discussion

Table 8 summarises the presently measured M2 strengths and compares them with previously published data. The strong M2 transitions in ^{22}Ne, ^{34}S and ^{35}Cl, already mentioned in table 1, are also included in this table. The present strengths for the transitions in ^{14}N, $^{16}O(12.97 \rightarrow 0$ MeV) and ^{21}Na clearly deviate from previous data. The present value for the $E_x = 12.53 \rightarrow 0$ MeV transition in ^{16}O agrees with one of the two conflicting values previously published.

Although several of the M2 strengths studied turn out to be weaker than previously reported, the reduction is insufficient to conclude to a lower RUL for isospin-allowed M2 transitions. This is due to the $E_x = 8.97 \rightarrow 0$ MeV transition in ^{14}N with $S_{M2} = 2.2 \pm 0.3$ W.u., which is now the strongest M2 transition known. For the $A = 6 - 44$ nuclei the isovector M2 RUL of 3 W.u. thus is justified.

Considering the significant differences between the present and the previous results it seems worthwhile to remeasure also the $S_{M2} = 1.6 \pm 0.5$ and 1.1 ± 0.3 W.u. transitions in ^{22}Ne and ^{34}S, respectively.

TABLE 8

Summary of the present results and comparison with previous data

Nucleus	$E_{xi} \rightarrow E_{xf}$ (MeV)	S_{M2} (W.u.)	
		present	literature [a])
^{14}N	8.91 → 0	2.2 ± 0.3	1.4 ± 0.5
^{16}O	12.97 → 0	1.0 ± 0.3	2.0 ± 0.1
^{16}O	12.53 → 0	1.12 ± 0.17	0.7 ± 0.2 [b]) or 3.7 ± 0.5 [c])
^{21}Na	2.80 → 0.33	< 0.4	1.1 ± 0.4
^{32}S	10.08 → 0	0.93 ± 0.13	1.3 ± 0.4
^{22}Ne	7.60 → 0		1.6 ± 0.4
^{34}S	5.68 → 2.13		1.1 ± 0.4
^{35}Cl	7.80 → 0	not M2 [d])	3.1 ± 1.0

[a]) Ref. [2]), unless indicated otherwise.
[b]) Ref. [6]).
[c]) Ref. [5]).
[d]) Ref. [4]).

We thank Joyce H.D.M. Westerink and Henk P.J. Schut for active help in data taking and analysis.

This work was performed as part of the research program of the "Stichting voor Fundamenteel Onderzoek der Materie" (FOM) with financial support from the "Nederlandse Organisatie voor Zuiver-Wetenschappelijk Onderzoek" (ZWO).

References

1) P.M. Endt and C. van der Leun, At. Data and Nucl. Data Tables **13** (1974) 67
2) P.M. Endt, At. Data and Nucl. Data Tables **23** (1979) 3
3) P.M. Endt, At. Data and Nucl. Data Tables **23** (1979) 547 and **26** (1981) 47
4) O.P. van Pruissen, G.J.L. Nooren and C. van der Leun, Nucl. Phys., to be published
5) J.C. Kim, R.P. Singhal and H.S. Caplan, Can. J. Phys. **48** (1970) 83
6) M. Stroezel, Z. Phys. **214** (1968) 357
7) F. Zijderhand and C. van der Leun, Verhandlungen DPG **18** (1982) 1032
8) J.W. Maas, E. Somorjai, H.D. Graber, C.A. van den Wijngaart, C. van der Leun and P.M. Endt, Nucl. Phys. **A301** (1978) 213
9) Y. Yoshizawa, Y. Iwata, K. Fukuhara and H. Inoue, At. Data and Nucl. Data Tables, to be published
10) F. Zijderhand and C. Alderliesten, Nucl. Instr. and Methods, to be published
11) F. Ajzenberg-Selove, Nucl. Phys. **A360** (1981) 1
12) F. Ajzenberg-Selove, Nucl. Phys. **A375** (1982) 1
13) P.M. Endt and C. van der Leun, Nucl. Phys. **A310** (1978) 1
14) G.J.L. Nooren and C. van der Leun, Nucl. Phys. **A423** (1984) 197
15) H.E. Gove, in Nuclear reactions, ed. P.M. Endt and M. Demeur, vol. 1 (North-Holland, Amsterdam, 1959) p. 259
16) W. Biesiot and P.B. Smith, Phys. Rev. **C24** (1981) 2443
17) H.G. Clerc and E. Kuphal, Z. Phys. **211** (1968) 452
18) A.G.M. van Hees, thesis, Rijksuniversiteit Utrecht (1982)
19) B.M. Paine and D.G. Sargood, Nucl. Phys. **A331** (1979) 389

20) E.E. Whiting, J. Quant. Spectrosc. and Radiat. Transfer **8** (1968) 1374
21) R.A. Leavitt, H.C. Evans, G.T. Ewan, H.-B. Mak, R.E. Azuma, C. Rolfs and K.P. Jackson, Nucl. Phys. **A410** (1983) 93
22) B. Maurel and G. Amsel, Nucl. Instr. **218** (1983) 159
23) H. Damjantschitsch, M. Weiser, G. Heusser, S. Kalbitzer and H. Mannsperger, Nucl. Instr. **218** (1983) 129
24) C. Rolfs, W.S. Rodney, M.H. Shapiro and H. Winkler, Nucl. Phys. **A241** (1975) 460
25) W.F. Coetzee, M.A. Meyer and D. Reitmann, Nucl. Phys. **A185** (1972) 644
26) E. Storm and H.I. Israel, Nucl. Data Tables **A7** (1970) 565